Structure, Volume *20*

Supplemental Information

Visualizing the Determinants of Viral RNA Recognition by Innate Immune Sensor RIG-I

Dahai Luo, Andrew Kohlway, Adriana Vela, and Anna Marie Pyle

Inventory of Supplemental Information

Supplementary Figures

Figure S1. Secondary folding of 5'ppp8L hairpin and panhandle-like viral genomic RNAs, related to Figure 1.

- 5'ppp8L hairpin

5' GG CGCGGCUUCG GCCGCG CC 3'

- gi|73919206|ref|NC_007366.1| Influenza A virus, segment 4.

5' AGCAAAAGCAG…TTGTTTCTACT 3'

- gi|19718363|ref|NC_003461.1| Human parainfluenza virus 1

5'ACCAAACAAG …CUUGUCUGGU 3'

- gi|9627197|ref|NC_001542.1| Rabies virus, complete genome

5' ACGCUUAACA … UGUUAAGCGU 3'

- gi|9629198|ref|NC_001781.1| Human respiratory syncytial virus

5' ACGCGAAAAA … UUUUUCUCGU 3'

- gi|10313991|ref|NC_002549.1| Zaire ebolavirus, complete genome

5' CGGACACACA … UGUGUGUCCA 3'

Figure S2. Crystal structures of RIG-I (ΔCARDs): dsRNA, related to Figure 1 and 2.

(A) Superposition of RIG-I (ΔCARDs 1-238): 5'ppp8L: ADP-Mg^{2+} (Yellow) and RIG-I (ΔCARDs 1-229): GC10: SO_4 (Blue). RMSD is 0.38 Å for 559 Cα atoms. (B) Superposition of known RIG-I: 5'tri-phosphorylated RNA complex. Red: RIG-I (ΔCARDs 1-238): 5'ppp8L: ADP-Mg^{2+}; Purple: RIG-I CTD and 5'ppp-dsRNA14 (PDB: 3LRN); Blue: RIG-I CTD and 5'ppp-dsRNA12 (PDB: 3NCU); Green: RIG-I CTD and 5'ppp-dsRNA12 (PDB: 3LRR). Among the structures, the closest distance between RIG-I and the γ phosphate is 3.7 Å (3LRR). (C) Fo-Fc omit map (green) and 2Fo-Fc (blue) map cover the 5'ppp8L hairpin, contoured at 3.0 and 1.0 σ respectively. (D) 2Fo-Fc electron density map at the ATPase active site is in blue and contoured at 1.0 σ.

Figure S3. 5'ppp8L stimulates ATP hydrolysis by RIG-I (blue) and RIG-I (ΔCARDs 1-238) (red), related to Figure 2 and Table S1.

Each data point is an average of triplicates. The ATPase assays were performed as described previously (Luo et al., 2011). For experiments varying ATP concentrations, 50 µl reaction mixtures (50 nM of protein, 5x NADH enzyme buffer, 25 mM MOPS pH 7.4, 10 mM $Mg(OAc)_2$, 30 mM K(OAc), 10 mM NaCl, 2 mM DTT and 400 nM RNA) were mixed with 0-5 mM ATP at 25 °C. The 5x enzyme buffer contained 1 mM NADH, 100 U of lactic dehydrogenase/ml, 500 U of pyruvate kinase/ml, and 2.5 mM phosphoenolpyruvate. Fluorescence readings (excitation, 340 nm; emission, 450 nm) were collected in Corning 96 well black half area flat bottom plates in a SpectraMax 250 plate reader. Initial velocities were calculated from a linear regression of each time course and corrected for background ATP hydrolysis and NADH oxidation. The initial velocities at varying ATP concentrations were plotted and fit to the Michaelis-Menten equation, $v0 = [Vmax \bullet [S]/(Km + [S])]$.

Figure S4. Binding of full-length RIG-I and CTD mutants to a triphosphorylated RNA duplex, related to Figure 1.

Amino acids within the CTD- triphosphate interaction network were mutagenized, and variants F853A and H847A expressed sufficiently well for biophysical studies. Affinity of the WT and mutant proteins were then studied using a calibrated electrophoretic mobility shift assay (EMSA) that has been used to quantitate the role of individual protein domains to recognition by RIG-I (Vela, A, submitted). The RNA ligand is a 14-mer RNA duplex, which is a length that binds RIG-I as a monomer(Luo et al., 2011), and which contains a single 5'-triphosphate at one end. The resultant K_d values were obtained: Full-length RIG-I = 168 ± 12.8 pM; RIG-I H847A = 1230 ± 68 pM; RIG-I F853A = 254 ± 19.6 pM. Error bars represent the standard deviation in three complete replicates of each binding curve. In the absence of a 5'-triphosphate, binding affinity of H847A to duplex RNA was not significantly different than that of WT, underscoring the role of this amino acid specifically in 5'-triphosphate recognition (data not shown). Data are consistent with previous analysis on the CTD domain protein by Wang *et al*(Wang et al., 2010).

Figure S1.

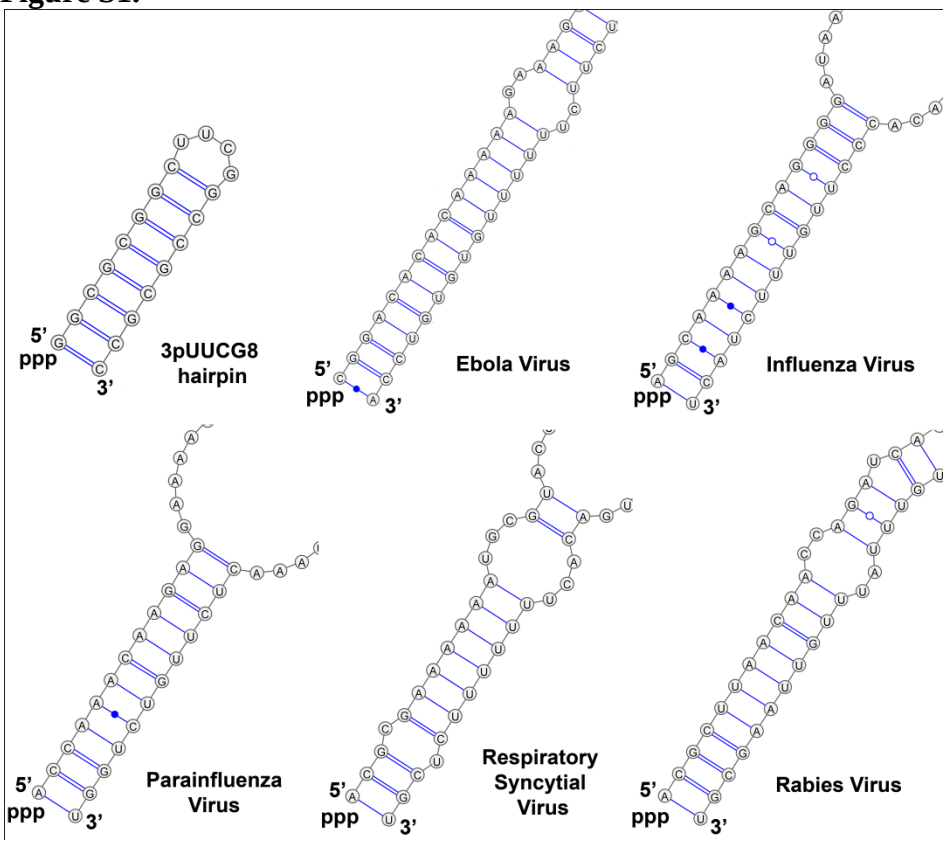
5'
ppp
3'
3pUUCG8
hairpin
Ebola Virus
Influenza Virus
Parainfluenza
Virus
Respiratory
Syncytial
Virus
Rabies Virus

Figure S2.
(A)

(B)

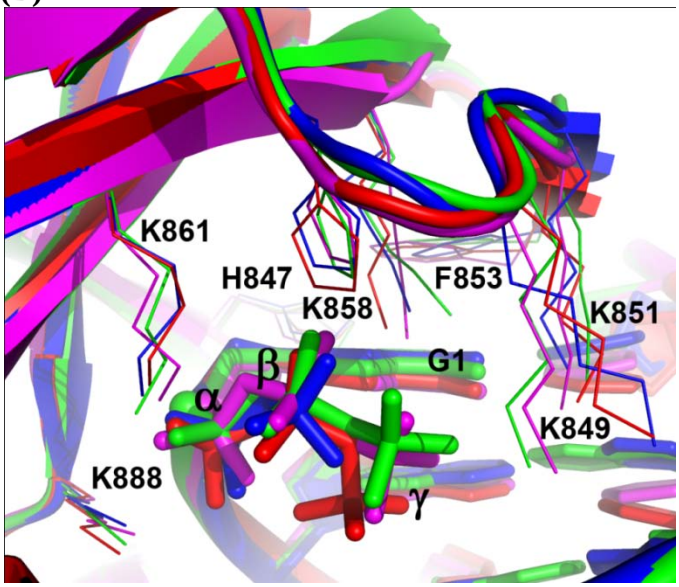

(C)

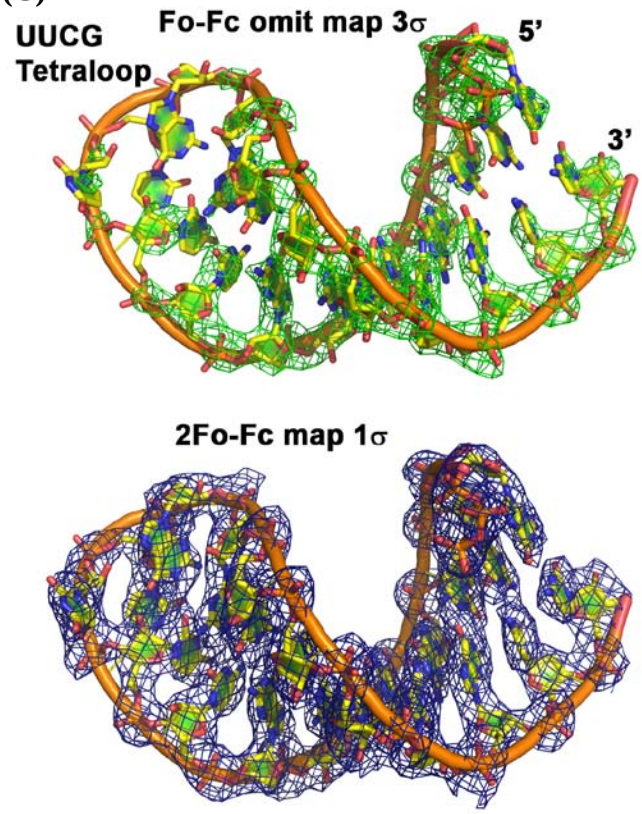
UUCG
Tetraloop
Fo-Fc omit map 3σ
5'
3'
2Fo-Fc map 1σ

(D)

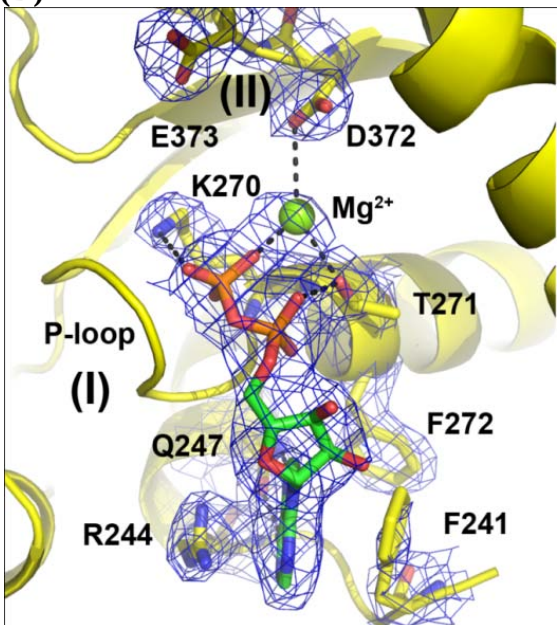
(II)
E373
D372
K270
Mg2+
T271
P-loop
(I)
F272
Q247
R244
F241

Figure S3.

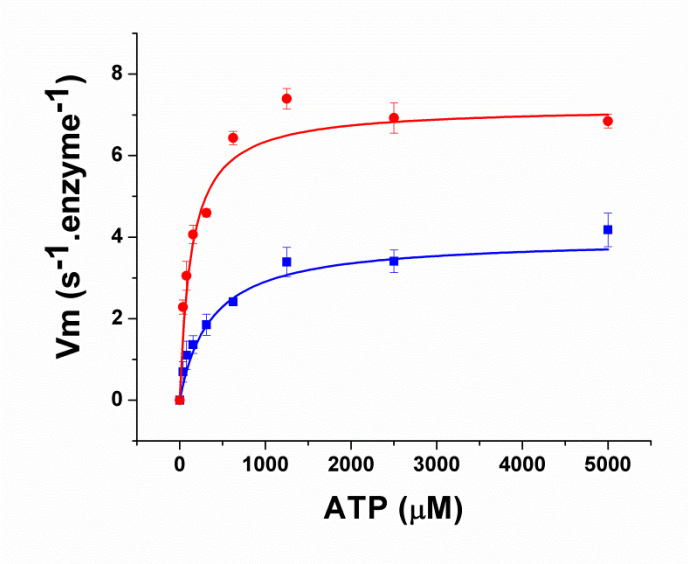

Figure S4.

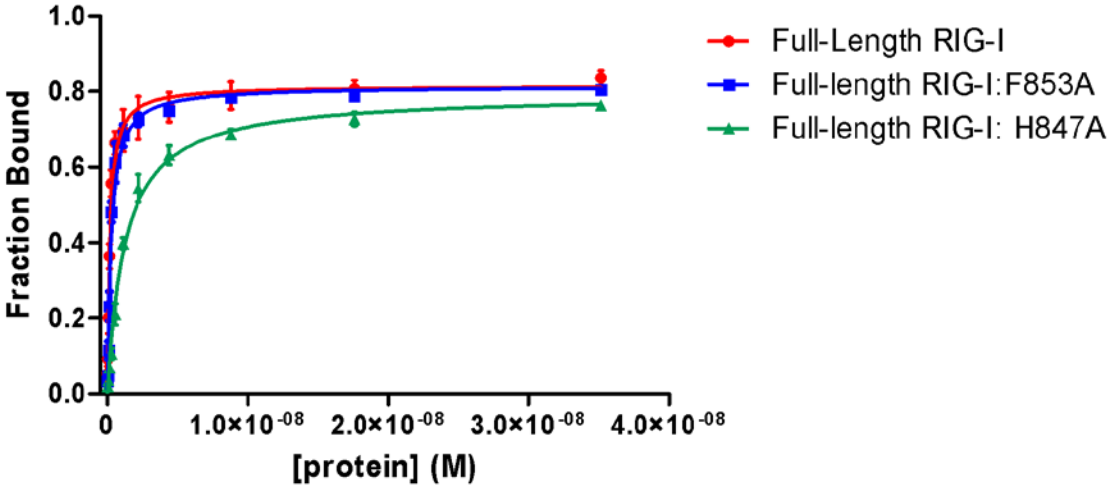
Fraction Bound
1.0
0.8
0.6
0.4
0.2
0.0
0
1.0×10-08
2.0×10-08
3.0×10-08
4.0×10-08
[protein] (M)
Full-Length RIG-I
Full-length RIG-I:F853A
Full-length RIG-I: H847A

Table S1. 5'ppp8L stimulated ATP hydrolysis by RIG-I, related to Figure 2, 3 and S3.

K_M (μM)	RIG-I (ΔCARDs 1-238)	RIG-I
	134.8 ± 31.4	365.2 ± 76.4
k_{CAT} (s^{-1}.enzyme^{-1})	RIG-I (ΔCARDs 1-238)	RIG-I
	7.2 ± 0.4	4.0 ± 0.3

References

Kowalinski, E., Lunardi, T., McCarthy, A. A., Louber, J., Brunel, J., Grigorov, B., Gerlier, D., and Cusack, S. (2011). Structural basis for the activation of innate immune pattern-recognition receptor RIG-I by viral RNA. Cell *147*, 423-435.
Luo, D., Ding, S. C., Vela, A., Kohlway, A., Lindenbach, B. D., and Pyle, A. M. (2011). Structural insights into RNA recognition by RIG-I. Cell *147*, 409-422.
Wang, Y., Ludwig, J., Schuberth, C., Goldeck, M., Schlee, M., Li, H., Juranek, S., Sheng, G., Micura, R., Tuschl, T., *et al.* (2010). Structural and functional insights into 5'-ppp RNA pattern recognition by the innate immune receptor RIG-I. Nat Struct Mol Biol *17*, 781-787.